ORGANOMETALLICS

pubs.acs.org/Organometallics

Communication

$[B(O_2C_2(CF_3)_4)_2]^-$ ([FPB]$^-$): Repurposing This Weakly Coordinating Anion for Solid-State Molecular Organometallic (SMOM) Chemistry

Kristof M. Altus, M. Arif Sajjad, Stuart A. Macgregor,* and Andrew S. Weller*

Cite This: https://doi.org/10.1021/acs.organomet.5c00112

Read Online

ACCESS | Metrics & More | Article Recommendations | Supporting Information

ABSTRACT: The perfluoropinacol borate-based anion $[B(O_2C_2(CF_3)_4)_2]^-$, [**FPB**]$^-$, is developed as a weakly coordinating anion for single-crystal to single-crystal organometallic solid/gas reactivity, resulting in the isolation and characterization (including periodic DFT and IGMH analysis) of the σ-alkane complex $[Rh(Cy_2PCH_2CH_2PCy_2)(exo\text{-}\eta^2\eta^2\text{-norbornane})][FPB]$. The synthetically useful solvent-free Na^+ salt, Na[FPB], and oxonium acid $[H(OEt_2)_2][FPB]$ are also reported.

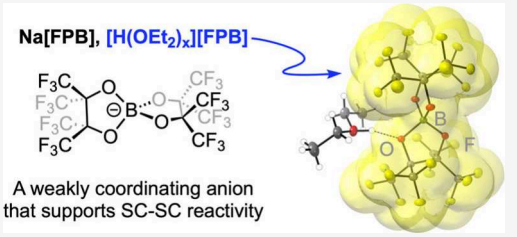

Weakly coordinating anions (WCAs) have been instrumental in the development of the synthetic and catalytic organometallic and main-group chemistry of reactive cationic species.[1−4] The ideal WCA should be chemically robust and of low polarizability, with the negative charge delocalized over a large surface area. While there are many different WCAs,[1] the most popular are based upon alkoxyaluminates, $[Al(OR^F)_4]^-$ (e.g., OR^F = $OC(CF_3)_3$, $OCH(CF_3)_2$),[5] or arylborates, e.g., $[BAr^F_4]^-$ (Ar^F = 3,5-$(CF_3)_2C_6H_3$),[6] Chart 1.

Chart 1. Common WCAs and the [FPB]$^-$ Anion

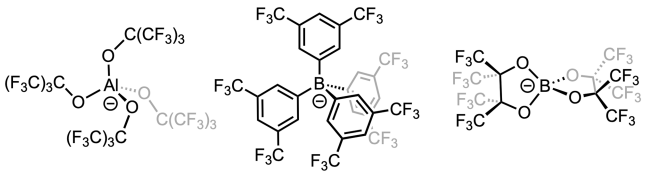

We have used the $[BAr^F_4]^-$ anion extensively in single-crystal to single-crystal (SC-SC) solid-state molecular organometallic chemistry (SMOM),[7−12] where partnering with a reactive transition metal cation allows for the isolation of solution-unstable complexes by solid/gas reactivity. For example, the stable σ-alkane complex $[Rh(Cy_2PCH_2CH_2PCy_2)(endo\text{-}\eta^2\eta^2\text{-NBA})][BAr^F_4]$ [**1-NBA**][**BAr$^F_4$**] (NBA = norbornane) results from reaction of a norbornadiene precursor with H_2.[7] The framework of $[BAr^F_4]^-$ anions supports metal-centered reactivity,[7−9] has CF_3 groups that promote substrate diffusion[13,14] and provides stability from noncovalent interactions.[9,10] In this system, different anions, such as $[Al(OR^F)_4]^-$[7] or $[B(3,5\text{-}Cl_2\text{−}C_6H_3)_4]^-$[15] either do not support SC-SC reactivity or result in NBA displacement to ultimately form an arene-coordinated zwitterion.

The multistep synthesis[16] of solvent-free precursor M-$[BAr^F_4]$ (M = Li^+, Na^+, K^+) creates a motivation to identify alternative anions that can facilitate SC-SC transformations. These anions should be cost-competitive and easily prepared on the gram scale as solvate-free salts of group 1 cations. The perfluoropinacol borate-based anion $[B(O_2C_2(CF_3)_4)_2]^-$, [**FPB**]$^-$ (Chart 1), offers these advantages. While its potential for use in organometallic chemistry has been suggested,[17] this has not been reported outside of a patent disclosing its use in olefin polymerization.[18] The stability of its group 1 salts, however, is demonstrated in its use as battery electrolytes.[19−21] We show here that [**FPB**]$^-$ can be used as a WCA for SMOM, by its use in the synthesis of a σ-alkane complex using SC-SC methods.

Solvate-free **Na**[**FPB**] is synthesized from commercial perfluoropinacol and $Na[BH_4]$ in THF solvent, using the reported method for group 1 cation salts, which have been structurally characterized as etherate solvates.[18−22] Heating the resulting solid under dynamic vacuum (10^{-2} mbar) at 80 °C (18 h) forms free-flowing powdered **Na**[**FPB**].[22] A single-crystal X-ray diffraction (SCXRD) study of **Na**[**FPB**] (crystals isolated from hot 1,2-dichloroethane) revealed a 1D coordination polymer with B−O···Na linkages, Scheme 1A. Solution NMR data[22] (THF-d_8) showed no significant resonances associated with THF-h_8 in the ^{1}H NMR spectrum. The cost of preparing **Na**[**FPB**] is competitive with Na-

Received: March 27, 2025
Revised: April 24, 2025
Accepted: April 28, 2025

Scheme 1. Synthesis of Na[FPB] and [H(OEt$_2$)$_2$][FPB]

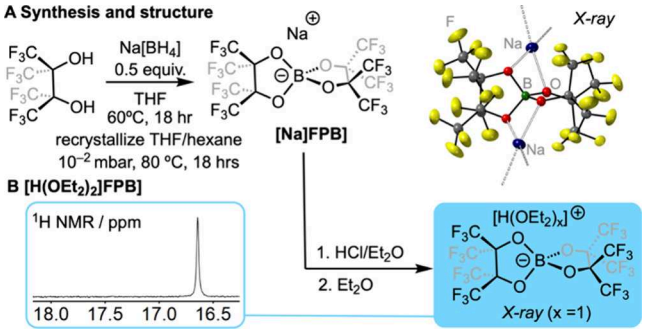

[BAr$^F_4$], ~£10 versus £7/mmol (January 2025 online prices); while the Process Mass Intensity metric (PMI) favors **Na**[**FPB**], 22.6 versus 52.6.[23] [**Caution!**] These advantages, however, should be balanced with the toxicity associated with the starting perfluoropinacol reagent;[24] see the Supporting Information.

The synthetically useful oxonium acid[6,25] [**H(OEt$_2$)$_2$**][**FPB**] can be prepared as a free-flowing white microcrystalline powder by addition of HCl to **Na**[**FPB**] in Et$_2$O solvent, following by filtration and removal of solvent [δ(^{1}H) = 16.6 *H*(OEt$_2$)$_2$, CD$_2$Cl$_2$], Scheme 1B. Addition of an excess of Proton Sponge (PS, 1,8-bis(dimethylamino)naphthalene) to [**H(OEt$_2$)$_2$**][**FPB**] resulted in a mixture of unchanged PS and [**PS-H**][**FPB**]/Et$_2$O, from which reliable integrals could be obtained in the ^{1}H NMR spectrum. This allows for the determination of Et$_2$O solvation of the oxonium acid in the bulk powder, i.e., [H(OEt$_2$)$_2$]$^+$. Analysis by SCXRD (crystals grown from CH$_2$Cl$_2$/Et$_2$O) revealed two polymorphs, one of which gave a solvable structure (Supporting Information). This reveals this polymorph to have only one Et$_2$O solvent molecule, which sandwiches the proton with the [**FPB**]$^-$ anion (see Figure S56).

The utility of **Na**[**FPB**] as a supporting anion for SC-SC solid−gas reactivity is demonstrated by the synthesis of [Rh(Cy$_2$PCH$_2$CH$_2$PCy$_2$)(NBD)][FPB], [**1-NBD**][**FPB**] (NBD = norbornadiene), and its onward solid/gas reactivity with H$_2$ to form the indefinitely stable σ-alkane complex [Rh(Cy$_2$PCH$_2$CH$_2$PCy$_2$)(*exo*-$\eta^2\eta^2$-NBA)][FPB], [**1-NBA**][**FPB**], Figure 1A. Complex [**1-NBD**][**FPB**] is isolated as block-like red crystals by a straightforward route using **Na**[**FPB**], [Rh(NBD)Cl$_2$]$_2$ and Cy$_2$PCH$_2$CH$_2$PCy$_2$. The SCXRD structure shows an orthobifastigium arrangement of [FPB]$^-$ anions surrounding two crystallographically equivalent [Rh(Cy$_2$PCH$_2$CH$_2$PCy$_2$)(NBD)]$^+$ cations, in which the NBD ligands are directed toward each other (Figure S52). Solution and solid-state NMR (SSNMR) data support this formulation. Addition of H$_2$ (1 bar) to crystals of [**1-NBD**][**FPB**] (50 mg scale) over 80 min results in the quantitative formation of [**1-NBA**][**FPB**] in a SC-SC transformation. The resulting ^{31}P{^{1}H} SSNMR spectrum shows a characteristic[7] downfield shift and increase in *J*(RhP) on formation of the σ-alkane complex (155 and 195 Hz), Figure 1B. In the ^{13}C{^{1}H} SSNMR spectrum of [**1-NBA**][**FPB**] signals due to NBD are absent, with broad signals due to the anion observed at δ 121.8 (vbr), 86.4 (br).

The SCXRD structure of [**1-NBA**][**FPB**] (Figure 1C) shows a NBA-alkane ligand binding through two 3c-2e Rh···H−C interactions [Rh···C 2.385(3) and 2.363(2) Å] to give a formally d^8, 16-electron Rh(I) center, similar to [**1-NBA**][**BAr$^F_4$**].[7] The H atoms associated with this interaction were located. However, in contrast with [**1-NBA**][**BAr$^F_4$**], the chelating NBA ligand binds through two *exo*-C−H groups, the same as observed for the metastable [**1-NBA**][**B(3,5-Cl$_2$-C$_6$H$_3$)$_4$**].[15] As for [**1-NBD**][**FPB**] the anions adopt an orthobifastigium arrangement (space group P-1, Figure 1D), and there is no significant change in the unit cell volume (3% difference). Uniquely for σ-alkane complexes synthesized using SMOM methods,[7−11] this packing directs the alkane ligands in the crystallographically equivalent cations to face one another, and the metal centers to be relatively close (~10 Å). As for [**1-NBA**][**BAr$^F_4$**], complex [**1-NBA**][**FPB**] is stable at 298 K under an Ar atmosphere (1 month by ^{31}P{^{1}H} SSNMR). It reacts rapidly with 1,2-F$_2$C$_6$H$_4$ solvent to displace the alkane to form the arene-adduct, [**1-F$_2$C$_6$H$_4$**][**FPB**],[11] as characterized by SCXRD (Figure 1E, Figure S54).

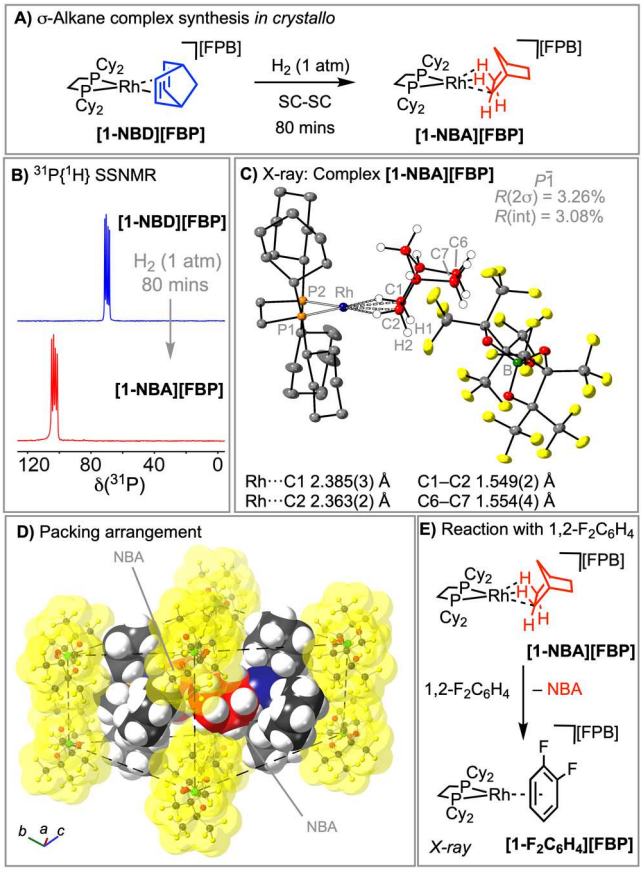

Figure 1. A) Synthesis of [**1-NBA**][**BAr$^F_4$**]. B) ^{31}P{^{1}H} SSNMR of [**1-NBD**][**BAr$^F_4$**] and [**1-NBA**][**BAr$^F_4$**]. C) Molecular structure of the asymmetric unit in [**1-NBA**][**BAr$^F_4$**]. Displacement ellipsoids at the 40% level. D) Packing arrangement of anions, van der Waals surface. E) Reaction of [**1-NBA**][**BAr$^F_4$**] with 1,2-F$_2$C$_6$H$_4$.

[**1-NBA**][**FPB**] was characterized computationally using periodic-DFT calculations. Geometry optimization relaxing the H atom positions shows elongation of the C1−H1A and C2−H2B bonds to 1.17 Å, and NBO calculations indicate dominant C−H → Rh σ-donation (Figure 2A). These, and other computed metrics (Figures S33−S36), all signal a σ-alkane complex. The η^2_{C-H} binding mode is also reflected in the computed Rh···H−C angles (102°) and the Independent Gradient Model plot based on Hirshfeld partitioning (IGMH, Figure 2B).

https://doi.org/10.1021/acs.organomet.5c00112
Organometallics XXXX, XXX, XXX−XXX

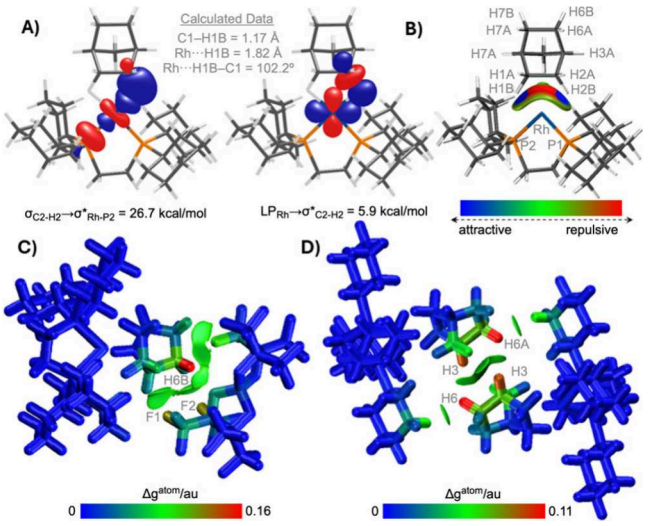

Figure 2. A) Key donor–acceptor interactions for the Rh-NBA interaction in the cation of [**1-NBA**][**FPB**] as quantified via second-order perturbation NBO analyses. B) IGMH plot for the cation highlighting the Rh-NBA interaction ($\text{sign}(\lambda_2)\rho$-colored isosurfaces with δG_{inter} = 0.003 au) C) IGMH plot of the cation–anion pair and D) IGMH plot of cation–cation pair (atoms colored by $\%\delta G^{atom}$). See Supporting Information for IGMH plots of other nearest-neighbor ion pairs.

The NBA solid-state binding energy in [**1-NBA**][**FPB**] (i.e., the energy required to remove one NBA ligand from the unit cell) is computed to be 49.5 kcal/mol and compares with a molecular binding energy (for the isolated cation) of 36.5 kcal/mol. This gives a solid-state stabilization energy (SSSE) of 12.5 kcal/mol, similar to that computed for the *endo*-bound NBA in [**1-NBA**][**BAr$^F_4$**] (14.0 kcal/mol).[9] For [**1-NBA**][**BAr$^{Cl}_4$**] (which also exhibits *exo*-NBA binding), the NBA solid-state binding energy is 50.7 kcal/mol, and the SSSE is 14.9 kcal/mol. Thus, the [BAr$^F_4$]$^-$ and [FPB]$^-$ lattices in [**1-NBA**][**BAr$^F_4$**] and [**1-NBA**][**FPB**] have similar influence on alkane binding across different topologies and NBA binding modes. In [**1-NBA**][**BAr$^{Cl}_4$**] the computed *exo* to *endo* rearrangement of one NBA ligand within the unit cell resulted in a destabilization of +2.3 kcal/mol. In [**1-NBA**][**FPB**] this is computed to be +8.4 kcal/mol, while in the absence of any solid-state environment this difference collapses to 0.3 kcal/mol. This emphasizes the role of the solid-state 2° microenvironment in controlling structure and stability.[26,27]

The role of the 2° microenvironment was further probed via IGMH plots of nearest neighbor ion pairs, in particular those highlighting interactions between the NBA ligand and the adjacent [**FPB**]$^-$ anion (Figure 2C) and between NBA ligands arising from the unusual back-to-back cation packing motif (Figure 2D). In both cases, green isosurfaces indicate regions of stabilizing dispersion interactions, while the atom color coding highlights the largest % atomic contributions in red. H6B···F1/F2 contacts contribute most to NBA···[**FPB**]$^-$ dispersion while the H3···H6A contacts are most prominent in the cation–cation pair. These interactions reflect correspondingly short computed nonbonded distances (H6A···F1 = 2.39 Å; H6A···F2 = 2.61 Å; H3···H7B = 2.49 Å). In total, forty-two short H···F contacts (i.e., $<\Sigma_{vdW\ radii}$[28] + 10%) are present around the cation in [**1-NBA**][**FPB**]. A further estimate of interion dispersion comes from the computed cation–anion interaction energies: with PBE+D3 these range from 32 to 68 kcal/mol and these drop by 5–15% when recomputed without the D3 correction (Figures S38–S45).

In conclusion, we show that the [**FPB**]$^-$ anion supports SC-SC solid/gas reactivity at reactive cationic metal centers. The ease of synthesis of a variety of synthetically useful salts, robustness, and low cost of [**FPB**]$^-$ mean that it perhaps should be considered more widely in the toolbox of organometallic and main-group chemistry more generally, when suitable precautions are taken for the safe handling of perfluoropinacol and its derivatives.

■ ASSOCIATED CONTENT

Supporting Information

The Supporting Information is available free of charge at https://pubs.acs.org/doi/10.1021/acs.organomet.5c00112.

Full experimental details, characterization, NMR spectra, cost analysis, computational details, electronic structure analyses, and X-ray crystallographic figures (PDF)

Computed geometries (XYZ)

Accession Codes

Deposition Numbers 2434355–2434359 contain the supplementary crystallographic data for this paper. These data can be obtained free of charge via the joint Cambridge Crystallographic Data Centre (CCDC) and Fachinformationszentrum Karlsruhe Access Structures service.

■ AUTHOR INFORMATION

Corresponding Authors

Stuart A. Macgregor – *EaStCHEM School of Chemistry, North Haugh, University of St. Andrews, St Andrews KY16 9ST, U.K.;* orcid.org/0000-0003-3454-6776; Email: sam38@st-andrews.ac.uk

Andrew S. Weller – *Department of Chemistry, University of York, York YO10 5DD, U.K.;* orcid.org/0000-0003-1646-8081; Email: andrew.weller@york.ac.uk

Authors

Kristof M. Altus – *Department of Chemistry, University of York, York YO10 5DD, U.K.;* orcid.org/0000-0002-8072-8346

M. Arif Sajjad – *EaStCHEM School of Chemistry, North Haugh, University of St. Andrews, St Andrews KY16 9ST, U.K.;* orcid.org/0000-0002-4119-9912

Complete contact information is available at: https://pubs.acs.org/10.1021/acs.organomet.5c00112

Notes

The authors declare no competing financial interest.

■ ACKNOWLEDGMENTS

EPSRC (EP/W015552/1 and EP/W015498/1). This work used the ARCHER2 UK National Supercomputing Service (https://www.archer2.ac.uk).[29]

■ REFERENCES

(1) Riddlestone, I. M.; Kraft, A.; Schaefer, J.; Krossing, I. Taming the Cationic Beast: Novel Developments in the Synthesis and Application of Weakly Coordinating Anions. *Angew. Chem., Int. Ed.* **2018**, *57*, 13982–14024.

(2) Bochmann, M. The Chemistry of Catalyst Activation: The Case of Group 4 Polymerization Catalysts. *Organometallics* **2010**, *29*, 4711–4740.

https://doi.org/10.1021/acs.organomet.5c00112
Organometallics XXXX, XXX, XXX–XXX

(3) Ittel, S. D.; Johnson, L. K.; Brookhart, M. Late-Metal Catalysts for Ethylene Homo- and Copolymerization. *Chem. Rev.* **2000**, *100*, 1169−1204.
(4) Engesser, T. A.; Lichtenthaler, M. R.; Schleep, M.; Krossing, I. Reactive p-block cations stabilized by weakly coordinating anions. *Chem. Soc. Rev.* **2016**, *45*, 789−899.
(5) Krossing, I. The Facile Preparation of Weakly Coordinating Anions: Structure and Characterisation of Silverpolyfluoroalkoxyaluminates $AgAl(OR^F)_4$, Calculation of the Alkoxide Ion Affinity. *Chem.—Eur. J.* **2001**, *7*, 490−502.
(6) Brookhart, M.; Grant, B.; Volpe, A. F., Jr. $[(3,5\text{-}(CF_3)_2C_6H_3)_4B]^-[H(OEt_2)_2]^+$: a convenient reagent for generation and stabilization of cationic, highly electrophilic organometallic complexes. *Organometallics* **1992**, *11*, 3920−3922.
(7) Pike, S. D.; Chadwick, F. M.; Rees, N. H.; Scott, M. P.; Weller, A. S.; Krämer, T.; Macgregor, S. A. Solid-State Synthesis and Characterization of σ-Alkane Complexes, $[Rh(L_2)(\eta^2,\eta^2\text{-}C_7H_{12})][BAr^F_4]$ (L_2 = Bidentate Chelating Phosphine). *J. Am. Chem. Soc.* **2015**, *137*, 820−833.
(8) Chadwick, F. M.; McKay, A. I.; Martinez-Martinez, A. J.; Rees, N. H.; Krämer, T.; Macgregor, S. A.; Weller, A. S. Solid-state molecular organometallic chemistry. Single-crystal to single-crystal reactivity and catalysis with light hydrocarbon substrates. *Chem. Sci.* **2017**, *8*, 6014−6029.
(9) Bukvic, A. J.; Burnage, A. L.; Tizzard, G. J.; Martínez-Martínez, A. J.; McKay, A. I.; Rees, N. H.; Tegner, B. E.; Krämer, T.; Fish, H.; et al. A Series of Crystallographically Characterized Linear and Branched σ-Alkane Complexes of Rhodium: From Propane to 3-Methylpentane. *J. Am. Chem. Soc.* **2021**, *143*, 5106−5120.
(10) Sajjad, M. A.; Macgregor, S. A.; Weller, A. S. A comparison of non-covalent interactions in the crystal structures of two σ-alkane complexes of Rh exhibiting contrasting stabilities in the solid state. *Faraday Discuss.* **2023**, *244*, 222−240.
(11) Chadwick, F. M.; Rees, N. H.; Weller, A. S.; Krämer, T.; Iannuzzi, M.; Macgregor, S. A. A Rhodium−Pentane Sigma-Alkane Complex: Characterization in the Solid State by Experimental and Computational Techniques. *Angew. Chem., Int. Ed.* **2016**, *55*, 3677−3681.
(12) Gyton, M. R.; Sajjad, M. A.; Storm, D. J.; Altus, K. M.; Goodall, J. C.; Johnson, C. L.; Page, S. J.; Edwards, A. J.; Piltz, R. O.; et al. An Operationally Unsaturated Iridium-Pincer Complex That C−H Activates Methane and Ethane in the Crystalline Solid-State. *J. Am. Chem. Soc.* **2025**, *147*, 8706−8719.
(13) Martínez-Martínez, A. J.; Rees, N. H.; Weller, A. S. Reversible Encapsulation of Xenon and CH_2Cl_2 in a Solid-State Molecular Organometallic Framework (Guest@SMOM). *Angew. Chem., Int. Ed.* **2019**, *58*, 16873−16877.
(14) Vitórica-Yrezábal, I. J.; Libri, S.; Loader, J. R.; Mínguez Espallargas, G.; Hippler, M.; Fletcher, A. J.; Thompson, S. P.; Warren, J. E.; Musumeci, D.; et al. Coordination Polymer Flexibility Leads to Polymorphism and Enables a Crystalline Solid−Vapour Reaction: A Multi-technique Mechanistic Study. *Chem.—Eur. J.* **2015**, *21*, 8799−8811.
(15) McKay, A. I.; Martínez-Martínez, A. J.; Griffiths, H. J.; Rees, N. H.; Waters, J. B.; Weller, A. S.; Krämer, T.; Macgregor, S. A. Controlling Structure and Reactivity in Cationic Solid-State Molecular Organometallic Systems Using Anion Templating. *Organometallics* **2018**, *37*, 3524−3532.
(16) Martínez-Martínez, A. J.; Weller, A. S. Solvent-free anhydrous Li^+, Na^+ and K^+ salts of $[B(3,5\text{-}(CF_3)_2C_6H_3)_4]^-$, $[BAr^F_4]^-$. Improved synthesis and solid-state structures. *Dalton Trans* **2019**, *48*, 3551−3554.
(17) Krossing, I.; Raabe, I. Noncoordinating Anions—Fact or Fiction? A Survey of Likely Candidates. *Angew. Chem., Int. Ed.* **2004**, *43*, 2066−2090.
(18) Gao, X.; Jaber, I. Novel Borate Activator. US Patent US20060009596A1, 2006.
(19) Ni, L.; Zhang, S.; Li, C.; Lu, J.; Li, J.; Wang, J.; Zhang, S.; Chen, G.; Zhang, Z.; et al. Tailored Cation−Anion Coordination in Carbonate Electrolyte Enabling a Rigid-Flexible Compact Solid-Electrolyte Interphase for Potassium Batteries. *Adv. Funct. Mater.* **2024**, *34*, 2400570.
(20) Chen, G.; Qiao, L.; Xu, G.; Li, L.; Li, J.; Li, L.; Liu, X.; Cui, Z.; Zhang, S.; et al. A Highly-Fluorinated Lithium Borate Main Salt Empowering Stable Lithium Metal Batteries. *Angew. Chem., Int. Ed.* **2024**, *63*, No. e202400797.
(21) Murugan, S.; Klostermann, S. V.; Frey, W.; Kästner, J.; Buchmeiser, M. R. A sodium bis(perfluoropinacol) borate-based electrolyte for stable, high-performance room temperature sodium-sulfur batteries based on sulfurized poly(acrylonitrile). *Electrochem. Commun.* **2021**, *132*, 107137.
(22) Ould, D. M. C.; Menkin, S.; Smith, H. E.; Riesgo-Gonzalez, V.; Jónsson, E.; O'Keefe, C. A.; Coowar, F.; Barker, J.; Bond, A. D.; et al. Sodium Borates: Expanding the Electrolyte Selection for Sodium-Ion Batteries. *Angew. Chem., Int. Ed.* **2022**, *61*, No. e202202133.
(23) Jimenez-Gonzalez, C.; Ponder, C. S.; Broxterman, Q. B.; Manley, J. B. Using the Right Green Yardstick: Why Process Mass Intensity Is Used in the Pharmaceutical Industry To Drive More Sustainable Processes. *Org. Process Res. Dev.* **2011**, *15*, 912−917.
(24) Perfluoropinacol should be treated as acutely toxic and is fatal if contacted with the skin. We can find no available data for the corresponding $[FPB]^-$ anion, despite its widespread adoption in battery research. We thank Professor Ingo Krossing (University of Freiburg) in alerting us to this paper: Laird, T. The Dangers of the Unknown. *Org. Process Dev.* **2003**, *7*, 225.
(25) Krossing, I.; Reisinger, A. Perfluorinated Alkoxyaluminate Salts of Cationic Brønsted Acids: Synthesis, Structure, and Characterization of $[H(OEt_2)_2][Al\{OC(CF_3)_3\}_4]$ and $[H(THF)_2][Al\{OC(CF_3)_3\}_4]$. *Eur. J. Inorg. Chem.* **2005**, *2005*, 1979−1989.
(26) Furfari, S. K.; Tegner, B. E.; Burnage, A. L.; Doyle, L. R.; Bukvic, A. J.; Macgregor, S. A.; Weller, A. S. Selectivity of Rh···H−C Binding in a σ-Alkane Complex Controlled by the Secondary Microenvironment in the Solid State. *Chem.—Eur. J.* **2021**, *27*, 3177−3183.
(27) Krämer, T.; Chadwick, F. M.; Macgregor, S. A.; Weller, A. S. Solid-State Confinement Effects in Selective exo-H/D Exchange in the Rhodium σ-Norbornane Complex $[(Cy_2PCH_2CH_2PCy_2)Rh(\eta^2{:}\eta^2\text{-}C_7H_{12})][BAr^F_4]$. *Helv. Chim. Acta* **2023**, *106*, No. e202200154.
(28) Alvarez, S. A cartography of the van der Waals territories. *Dalton Trans.* **2013**, *42*, 8617−8636.
(29) Beckett, G.; Beech-Brandt, J.; Leach, K.; Payne, Z.; Simpson, A.; Smith, L.; Turner, A.; Whiting, A. *ARCHER2 Service Description*; Zenodo, 2024, DOI: 10.5281/zenodo.14507040.

https://doi.org/10.1021/acs.organomet.5c00112
Organometallics XXXX, XXX, XXX−XXX